



27 **ABSTRACT**

28 The ongoing COVID-19 pandemic has seen an unprecedented increase in the demand for  
29 rapid and reliable diagnostic tools, leaving many laboratories scrambling for resources. We  
30 present a fast and simple method for the detection of SARS-CoV-2 in nasopharyngeal swabs.  
31 The method is based on the detection of SARS-CoV-2 nucleoprotein (NP) and S protein (SP)  
32 via time-resolved Förster resonance energy transfer (TR-FRET) with donor- and acceptor-  
33 labeled polyclonal anti-NP and -SP antibodies. Using recombinant proteins and cell culture-  
34 grown SARS-CoV-2 the limits of detection were established as 25 pg of NP or 20 infectious  
35 viral units (i.u.), and 875 pg of SP or 625 i.u. of SARS-CoV-2. Testing RT-PCR positive (n=48,  
36 with cycle threshold [Ct] values from 11 to 30) or negative (n=96) nasopharyngeal swabs, we  
37 showed that the assay yields positive results for all samples with Ct values of <25 and a single  
38 RT-PCR negative sample. We determined the presence of infectious virus in the RT-PCR-  
39 positive nasopharyngeal swabs by virus isolation, and observed a strong association between  
40 the presence of infectious virus and a positive antigen test result. The NP-based assay showed  
41 97.4% (37/38) sensitivity and 100% (10/10) specificity in comparison with virus isolation, and  
42 77.1% (37/48) and 99.0% (95/96) in comparison with SARS-CoV-2 RT-PCR. The assay is  
43 performed in a buffer that neutralizes SARS-CoV-2 infectivity and is relatively simple to set  
44 up as an “in-house” test. The assay principle as such is applicable to other viral infections, and  
45 could also be readily adapted to a massively high throughput testing format.

## 46 INTRODUCTION

47 The ongoing coronavirus disease 2019 (COVID-19) pandemic has by December 2020  
48 claimed almost one and a half million lives globally, with over 60 million confirmed infections.  
49 To manage the disease, accurate diagnostic tools are of key importance. Detection of the  
50 causative agent, the severe acute respiratory syndrome coronavirus 2 (SARS-CoV-2), or its  
51 parts is the cornerstone of diagnosis, as the disease presentation is often indistinguishable from  
52 other respiratory infections. The mainstay of COVID-19 diagnosis is RT-PCR testing, done  
53 typically from a nasopharyngeal swab (NPS), while also oropharyngeal or mid-turbinate swab  
54 as well as salivary samples are in use. Alternatively, the less labour-intensive antigen detection  
55 tests are also increasingly deployed. Antigen tests tend to be specific, but analytically less  
56 sensitive than RT-PCR. RT-PCR can detect viral nucleic acid even after the infectious virus  
57 has waned, with the individual at this time unlikely posing a transmission risk<sup>1-3</sup>. Evidence  
58 suggests that antigen testing may correlate with recovery of infectious virus better than a binary  
59 RT-PCR<sup>4</sup>. Frequent antigen testing has been proposed as an alternative approach in reducing  
60 community transmission of SARS-CoV-2<sup>5</sup>.

61 SARS-CoV-2 is an enveloped (+)ssRNA virus of genus *Betacoronavirus* in family  
62 *Coronaviridae* of the *Nidovirales* order. It contains four structural proteins: the nucleoprotein  
63 (NP) forms a ribonucleoprotein complex with the 30 kb non-segmented viral genome. The  
64 envelope (E) and membrane (M) proteins are embedded in the envelope, as is the spike protein  
65 (SP), protruding from the virion surface and generating large surface projections termed the  
66 corona. The SP undergoes processing to yield S1, which contains the receptor-binding domain  
67 (RBD) initially attaching the virus to angiotensin-converting enzyme-2 (ACE-2) on the host  
68 cell membrane, and S2 that mediates virus-cell fusion. In response to the pandemic, dozens of  
69 commercial SARS-CoV-2 antigen tests are available, predominantly of lateral flow or enzyme  
70 immunoassay type. Most target NP as analyte<sup>6</sup>. Of the seven antigen tests having by December

71 2020 received emergency use authorization (EUA) from the U.S. Food and Drug  
72 Administration (FDA), six target N and one S<sup>7</sup>.

73 Over the past few years, we have actively employed time-resolved Förster resonance energy  
74 transfer (TR-FRET) as basis of rapid homogeneous “mix and read” immunoassays for antibody  
75 detection<sup>8-14</sup>. FRET occurs when a donor and an acceptor fluorophore are in close proximity,  
76 whereby the excited donor transfers energy to the acceptor, which then emits a photon at a  
77 distinct wavelength. The closer the donor and acceptor are, the more frequent is the energy  
78 transfer, with a 50% efficiency typically achieved at a distance of 15 to 60 Å. Chelated  
79 lanthanide donor-enabled TR-FRET allows for measurement from autofluorescent biological  
80 samples.

81 Herein, we describe a rapid TR-FRET -based method for detection of SARS-CoV-2 NP and  
82 SP. In the assay polyclonal anti-NP and anti-RBD rabbit antibodies, each labeled with either a  
83 donor or an acceptor fluorophore, are combined at equimolar ratio and mixed with the clinical  
84 sample. The antigen, if present, binds the labeled antibodies and brings the fluorophores to  
85 close proximity. This results in a TR-FRET signal upon excitation, indicating presence of the  
86 antigen. We initially demonstrate the limits of detection for recombinant NP and SP as well as  
87 cell culture-grown SARS-CoV-2. We then evaluate the assay performance among 48 RT-PCR  
88 positive and 96 negative clinical NPS samples, and compare the antigen detection results to  
89 those of RT-PCR and virus cultivation.

## 90 **MATERIALS AND METHODS**

### 91 **Patient samples and reference results**

92 The evaluation of the SARS-CoV-2 TR-FRET assay was conducted by using  
93 nasopharyngeal swab (NPS) specimens collected in saline. The specimens were retrieved from  
94 patients with a clinically suspected COVID-19 and they were originally sent to HUS Diagnostic  
95 Center, HUSLAB for SARS-CoV-2 RT-PCR testing. The specimens were subsequently stored  
96 at -20°C.

97 The SARS-CoV-2 RT-PCR was based on a laboratory-developed test (LDT). The details  
98 and performance of the test in our laboratory setting have been described previously<sup>15</sup>. In this  
99 method (based on the N-gene, modified from Corman et al.<sup>16</sup>), the specimens were inactivated  
100 by combining 250 µl of MagNA Pure Lysis/Binding Buffer (Roche Diagnostics GmbH,  
101 Mannheim, Germany) and 250 µl of the specimen. Nucleic acid extraction was done from 450  
102 µl specimen lysate with the MagNA Pure Viral NA SV 2.0 Kit (Roche Diagnostics GmbH,  
103 Mannheim, Germany). RT-PCR was performed using the SuperScript III Platinum One-Step  
104 qRT-PCR Kit with 600 nM of the forward primer CACATTGGCACCCGCAATC, 800 nM of  
105 the reverse primer GAGGAACGAGAAGAGGCTTG and 200 nM of the probe FAM-  
106 ACTTCCTCAAGGAACAACATTGCCA-BBQ3.

107 The SARS-CoV-2 RT-PCR positive panel comprised 48 specimens with cycle threshold  
108 (Ct) values ranging linearly between 11.42 and 29.98 in the LDT. The SARS-CoV-2 RT-PCR  
109 negative panel comprised 96 samples negative in the LDT. Patient data were collected and  
110 samples handled according to research permit approved by the local review board, permit  
111 HUS/32/2018 (Helsinki University Hospital, Finland).

### 112 **Cell lines, virus isolation and propagation**

113 Vero E6 cells were transduced with a lentiviral vector expressing human Transmembrane  
114 serine protease 2, TMPRSS2, transcript variant 2 cDNA (NM\_005656.4) and as selection

115 marker blasticidin. Specifically, 1 ml of 0.22  $\mu\text{m}$  filtered (Millipore) infectious supernatant of  
116 HEK293T cells transfected on a 10-cm plate 48 h earlier using 30  $\mu\text{g}$  polyethylenimine with 5  
117  $\mu\text{g}$  pLenti6.3/V5-DEST TMPRSS2 (obtained from Biomedicum Functional Genomics Unit,  
118 University of Helsinki), and 5  $\mu\text{g}$  p8.9NDSB<sup>17</sup> plus 2-5  $\mu\text{g}$  of pMD2.G (a gift from Didier  
119 Trono, Addgene plasmid #12259; <https://n2t.net/addgene:12259>; RRID:Addgene\_12259) was  
120 added on Vero E6 cells seeded onto 6-well plates. Following 2 days of selection with 15  $\mu\text{g}/\text{ml}$   
121 of Blastidicin S HCl (Invitrogen), the cells were allowed to expand until confluency, and were  
122 subcultured three times. Once confirmed p24 negative, a clonal population of Vero E6-  
123 TMPRSS2 cells was obtained by limiting dilution. The obtained clones (N=5) were analyzed  
124 for TMPRSS2 expression by immunoblotting with V5 antibody (Invitrogen). The clone  
125 expressing the highest amount of TMPRSS2, VE6-TMPRSS2-H10, was selected for use.

126 SARS-CoV-2 isolation from clinical samples (stored at  $-20^{\circ}\text{C}$  since the day of collection,  
127 not subjected to freeze-thaw) was attempted on both Vero E6 and VE6-TMPRSS2-H10 cells.  
128 Both cell lines were cultivated in Minimal Essential Medium Eagle (MEM, Sigma)  
129 supplemented with 10% fetal bovine serum (FBS, Gibco), 100 IU penicillin and 100  $\mu\text{g}/\text{ml}$   
130 streptomycin (Sigma), and 2 mM L-glutamine (Sigma). For isolation, the cells were grown on  
131 12-well plates until approximately 90% confluent, the growth medium replaced with 400  $\mu\text{l}$  of  
132 MEM-2% (as above but with 2% FBS), followed by addition of 50  $\mu\text{l}$  of the NPS sample (under  
133 biosafety level 3 conditions), and 1 h incubation at  $37^{\circ}\text{C}$  5%  $\text{CO}_2$ . After two washes with MEM-  
134 2%, cultures were kept in 1 ml fresh MEM-2% for 4 days at  $37^{\circ}\text{C}$  (5%  $\text{CO}_2$ ), the medium  
135 collected and clarified by centrifugation (3,000 x rcf, 5 min), and the cells fixed for 15 min at  
136 room temperature by 3.7% formaldehyde in phosphate-buffered saline (PBS) followed by PBS  
137 wash and UV inactivation (5,000 x100 mJ, UV Crosslinker, CL-1000, Jena Analytik). The  
138 fixed cells were Crystal violet stained, and the extent of cytopathic effect (CPE) scored from 0  
139 to 3 (from non-observable to extensive cell death). To confirm infection, RNA was extracted

140 (QIAgen QIAamp Viral RNA Extraction Kit, following manufacturer's protocol) from 100  $\mu$ l  
141 of each cell culture supernatant, and the presence or absence of SARS-CoV-2 analyzed by RT-  
142 PCR targeting the RdRp (RNA-dependent RNA polymerase) gene as described<sup>16</sup>.

143 For TR-FRET antigen detection experiments, we produced a stock of SARS-CoV-2 in Vero  
144 E6 cells<sup>18</sup>. Briefly, 90-95% confluent Vero E6 cells were inoculated with 500  $\mu$ l of 1:100  
145 diluted SARS-CoV-2 containing supernatant (passage 7, approximately  $5 \times 10^7$  tissue culture  
146 infectious dose 50, TCID<sub>50</sub>, per ml). After 1 h of virus adsorption, the medium was replaced  
147 with MEM-2%, and after 2 days at 37°C 5% CO<sub>2</sub>, the supernatant collected and clarified by  
148 centrifugation (3,000 x rcf, 5 min), and stored in aliquots at -80°C. UV inactivation of culture  
149 supernatants was done as described above.

150 Human coronavirus 229E (hCoV-229E, kindly provided by Dr. Sisko Tauriainen,  
151 University of Turku, Turku, Finland) and NL63 (hCoV-NL63, kindly provided by Lia van der  
152 Hoek, Academic Medical Center, Amsterdam, Netherlands) served as controls for estimating  
153 cross-reactivity of the assay. The hCoV-229E stock was produced by inoculating rhesus  
154 macaque kidney cells, LLC-MK2 (from ATCC), with 500  $\mu$ l of 1:1000 diluted cell culture  
155 supernatant (approximately  $5 \times 10^9$  TCID<sub>50</sub>/ml) 1 h at 37°C 5% CO<sub>2</sub>. After virus adsorption,  
156 the medium was changed into MEM-2%, the cells grown for 5 d (37°C, 5% CO<sub>2</sub>), the  
157 supernatant collected, centrifuged (3,000 x rcf, 5 min), and stored in aliquots at -80°C. The  
158 hCoV-NL63 stock was produced by inoculating human lung fibroblasts (MRC-5, from ATCC)  
159 with 500  $\mu$ l of 1:100 diluted cell culture supernatants (approximately  $1 \times 10^6$  TCID<sub>50</sub>/ml) for  
160 1 h at 37°C 5% CO<sub>2</sub>. After virus adsorption, the media were replaced with MEM-2%, the cells  
161 grown for 7 d (until appearance of definitive CPE), supernatants collected, centrifuged (3,000  
162 x rcf, 5 min) and stored in aliquots at -80°C. The hCoV-229E and hCoV-NL63 supernatants  
163 were inactivated for the experiments by mixing at 1:10 in RIPA buffer (50 mM Tris-HCl pH

164 8.0, 150 mM NaCl, 1% NP-40, 0.1% SDS, 0.5% sodium deoxycholate and Roche cComplete  
165 EDTA-free protease inhibitor cocktail).

### 166 **Antigens and antibodies**

167 The production and purification of SARS-CoV-2 NP and SP antigens, followed a described  
168 protocol<sup>14,19,20</sup>. The RBD of the SP was produced in Expi293F cells as described<sup>19,20</sup>. Rabbit  
169 antisera against RBD and NP were generated at BioGenes GmbH (Berlin, Germany): day 0  
170 initial dose 150 µg, day 7 booster 75 µg, day 14 booster 75 µg, day 28 booster 150 µg, and day  
171 42 final bleed. For affinity purification, RBD and NP were coupled to CNBr-Sepharose 4B  
172 (Cytiva) following the manufacturer's protocol. The respective antisera were passed through  
173 coupled Sepharoses packed into Poly-Prep Chromatography Columns (Bio-Rad), washed with  
174 20 column volumes of phosphate-buffered saline (PBS), eluted (0.1 M glycine, 150 mM NaCl,  
175 pH 2.5) with 2 M Tris, pH 9.0, concentrated using Amicon Ultra 15 ml 100 kDa-NMWL  
176 Centrifugal Filter (Millipore/Merck), and dialyzed against PBS using Slide-A-Lyzer Dialysis  
177 Cassettes (Thermo Scientific).

### 178 **Labelling**

179 We labelled the affinity-purified antibodies, 250 µg/reaction, with donor (europium, Eu)  
180 and acceptor (Alexa Fluor 647, AF647) respectively using QuickAllAssay Eu-chelated protein  
181 labeling kit (BN Products and Services Oy) and Alexa Fluor™ 647 NHS Ester (Thermo  
182 Scientific) following the manufacturer's instructions. Disposable PD-10 Desalting Column  
183 with Sephadex G-25 resin (Cytiva) served to remove non-reacted fluorophores, and Amicon  
184 Ultra 0.5 ml 50 kDa-NMWL Centrifugal Filter (Millipore/Merck) for concentrating the  
185 labelled antibodies, which were then stored aliquoted at -80°C until use.

### 186 **TR-FRET assays**

187 First, we set up TR-FRET assays for SARS-CoV-2 SP and NP antigens, by using the  
188 respective purified proteins as well as the corresponding Eu- and AF-labeled anti-RBD and



189 anti-NP antibodies. The assay principle and workflow are depicted in Fig. 1. Briefly, antibody  
190 mixes with equimolar concentrations of Eu- and AF-labeled anti-RBD and anti-NP antibody  
191 concentrations were prepared in RIPA buffer. For setting up the assay, a pool of four SARS-  
192 CoV-2 negative NPS samples was divided in aliquots and spiked with either NP or SP proteins  
193 at various concentrations. 10  $\mu$ l of antibody mix was pipetted on a 384-well microplate  
194 (ProxiPlate 384 Plus F, Black 384-shallow well microplate, PerkinElmer, USA), followed by  
195 10  $\mu$ l of the antigen-spiked sample. TR-FRET signal was measured directly thereafter and at  
196 time points 7, 15, 22, 30, 45, 60 and 90 minutes after the first measurement with a Hidex Sense  
197 microplate reader (Hidex Oy, Finland). FRET donor excitation was done at 330 nm and after a  
198 delay of 70  $\mu$ s the donor and acceptor signals were measured for 100  $\mu$ s at 616 and 665 nm,  
199 respectively. TR-FRET signals were expressed as HTRF ratios, calculated as follows: HTRF  
200 ratio = emission at 616 nm / emission at 665 nm x 10000. Thereafter, the HTRF ratios measured  
201 from the antigen-spiked samples were compared with those measured from a non-spiked  
202 sample in the same run to calculate the fold increase in HTRF ratio. Antibody plate  
203 concentrations ranging from 5 to 500 nM (half Eu- and half AF-labeled) were cross-titrated  
204 with antigen plate concentrations ranging from 5 nM to 500 nM.

205 The ranges of antigen concentrations detectable by TR-FRET (at Eu- and AF-labeled anti-  
206 NP/-RBD concentrations of 6 + 6 nM) were then assessed by performing the assay as described  
207 above using N and S plate concentrations of 5 fM to 5 nM.

208 To assess the assay performance with samples containing virions, cell culture supernatants  
209 containing roughly  $10^7$  TCID<sub>50</sub>/ml of SARS-CoV-2 were used. For initial experiments (carried  
210 out in BSL-3 laboratory) infectious cell culture supernatant (undiluted, 1:10, 1:25, 1:50, and  
211 1:100 diluted in RIPA) was used. After verifying that UV inactivated virus produced similar  
212 results, the negative NPS sample matrix was spiked with UV-inactivated virus-containing cell  
213 culture supernatant to yield a dilution series from 1:10 to 1:20480. The samples were tested in

214 the TR-FRET assays performed as above at Eu- and AF-labeled anti-NP/-RBD concentrations  
215 of 6 + 6 nM.

216 The NPS sample analysis was done by mixing 10  $\mu$ l of the sample with 10  $\mu$ l of the antibody  
217 mixes (Eu- and AF-labeled anti-NP/-RBD concentrations of 6 + 6 nM). The TR-FRET assays  
218 with SARS-CoV-2 RT-PCR positive NPS samples were carried out in BSL-3 laboratory and  
219 RT-PCR negative samples in BSL-2 laboratory. The signals produced by hCoV-229E and  
220 hCoV-NL63 were evaluated by mixing 10  $\mu$ l (undiluted, 1:10, 1:25, 1:50, and 1:100 diluted in  
221 RIPA) of the cell culture supernatant with 10  $\mu$ l of the antibody mixes (at Eu- and AF-labeled  
222 anti-NP/-RBD concentrations of 6 + 6 nM).

## 223 **RESULTS**

### 224 **Proof-of-concept for the homogeneous antigen detection assay**

225 We hypothesized that homogenous i.e. in solution detection of antigens could be achieved  
226 utilizing a polyclonal antibody separately labelled with fluorophores forming a FRET pair. To  
227 test the hypothesis and assay principle presented in Fig. 1, we generated antisera against SARS-  
228 CoV-2 NP and the RBD of SP, titers >204,800 based on NP and SP ELISA respectively.  
229 Following affinity purification, the antibodies were labelled with chelated europium (Eu,  
230 donor) and AlexaFluor 647 (AF647, acceptor). In the first experiments, we tested the assay  
231 principle by mixing recombinant NP and SP with 1  $\mu$ M (500 nM nM Eu labelled + 500 nM  
232 AF647 labelled) anti-NP and anti-RBD antibody mixtures in the presence of increasing bovine  
233 serum albumin (BSA) concentrations. Addition of BSA increased the signal-to-noise ratio,  
234 encouraging us to evaluate the assay performances further utilizing infectious SARS-CoV-2  
235 containing cell culture supernatants and different buffer compositions. The assay with 1  $\mu$ M  
236 antibody concentrations produced respectable signal-to-noise ratios in detergent-containing  
237 RIPA (radioimmunoprecipitation assay) buffer (Fig. S1). RIPA buffer (refer to materials and  
238 methods for the full recipe) used here contained 1% NP-40 and 0.1% SDS, both shown to  
239 effectively inactivate the enveloped SARS-CoV-2<sup>21,22</sup>, which is why we to employ RIPA for  
240 the subsequent analyses.

### 241 **Assay optimization using recombinant antigens and SARS-CoV-2**

242 To optimize the assay performance, we mixed the labelled antibodies at equimolar ratio with  
243 known amounts of recombinant NP and SP, and recorded the produced TR-FRET signals (as  
244 HTRF, homogeneous time-resolved fluorescence, values) as a function of time. The results  
245 showed the assays to produce the highest HTRF values when the concentration of labeled  
246 antibodies equalled the concentrations of the purified respective antigens (Fig. S2). Higher  
247 antibody concentrations shortened the time required for reaching the signal peak (fold increase  
248 in HTRF value,  $\text{HTRF}_{\text{sample}}/\text{HTRF}_{\text{buffer}}$ ): In an antibody concentration of 5 nM (2.5 nM Eu- +

249 2.5 nM of AF647-labeled) it took ~60 min for the signal to peak for both NP and SP, whereas  
250 in an antibody concentration of 500 nM, the NP signal peak occurred in 7 min and the SP signal  
251 peaked in ~30 minutes. We also tested the assay performances with Eu- and AF-labeled  
252 antibodies mixed at the unequal proportions of 1:2 and 2:1, but this did not increase the signal  
253 to background ratio (Table S1).

254 We then evaluated the assay performance at 50, 25, 12, and 6 nM total antibody  
255 concentrations using SARS-CoV-2 containing cell culture supernatants at different dilutions.  
256 We included a UV-inactivated cell culture supernatant to find out whether UV inactivation  
257 would affect the analysis. The results concurred with the findings using recombinant antigens,  
258 and showed the dependence of the TR-FRET signal kinetics on the antigen concentration (Fig.  
259 S3). The results further indicated that 12 nM total antibody concentration enables measurement  
260 of antigens over a broad range of virus concentrations, and that infectious and UV-inactivated  
261 SARS-CoV-2 produce similar results.

## 262 **Limits of detection**

263 To assess the limits of detection (LOD) for the assays at 12 nM total antibody concentration,  
264 we spiked a pool of NPS samples with either purified antigens or inactivated SARS-CoV-2 at  
265 different dilutions. With purified antigens, the lowest concentrations producing readily  
266 detectable signals were 0.05 nM for NP and 0.5 nM for SP (Fig. S4, a-b). With UV-inactivated  
267 SARS-CoV-2, dilutions of the supernatant up to 1:5120 and 1:160 produced reliably  
268 measurable signals with anti-NP and anti-RBD antibodies, respectively (Fig. S4, c-d). With the  
269 10  $\mu$ l sample volume, the detection limit of the assay for recombinant NP was ~25 pg (using  
270 molecular weight of 50 kDa) and 875 pg for the SP (using molecular weight of 175 kDa).  
271 Correspondingly, the NP assay could detect approximately 15 and the RBD assay  
272 approximately 420 plaque-forming units (converted by using  $0.7 \times \text{TCID}_{50}/\text{ml} = \text{pfu}/\text{ml}$ ) per  
273 reaction.

## 274 **Detection of SARS-CoV-2 antigens in NPS samples**

275 After setting up the assay conditions using recombinant proteins and cell culture grown  
276 virus, we tested the assays in detection of viral antigen in SARS-CoV-2 RT-PCR positive NPS  
277 samples. We had 48 NPS samples with RT-PCR cycle threshold (Ct) values linearly ranging  
278 from ~12 to 30 (Fig. S5), and employed total antibody concentrations of 50, 25, 12, and 6 nM.  
279 We observed that samples with Ct values of  $\leq 25$  yielded a signal in the NP assay (Fig. S6). By  
280 using the optimized conditions with 12 nM total labeled antibodies, the sensitivity of NP TR-  
281 FRET assay in comparison with RT-PCR was 77.1% (37/48). The SP assay showed greater  
282 diversity; most samples with Ct values  $\leq 15$  yielded a positive result (Fig. S6). We also  
283 performed an immunoblot to detect NP and SP in NPS samples covering the Ct value range of  
284 12.8 to 26.2, and could detect SP and NP in samples with Ct value  $< 22$  (Fig. S7).

## 285 **Association between infectious virus and antigen detection**

286 To determine to what extent the antigen assays correspond to the amounts of infectious virus  
287 in the sample, we subjected the 48 SARS-CoV-2 RT-PCR positive NPS samples to virus  
288 isolation. Transmembrane serine protease 2 (TMPRSS2) has been reported to function in  
289 priming the SARS-CoV-2 spike for entry<sup>23</sup>, and we thus chose to use both wild-type and a  
290 clonal population of TMPRSS2 expressing (VE6-TMPRSS2-H10) Vero E6 cells (Fig. S8). As  
291 indicated by cytopathic effects as well as RT-PCR from the cell culture supernatants, SARS-  
292 CoV-2 was isolated from 35/48 and 38/48 NPS samples with Vero E6 and VE6-TMPRSS2-  
293 H10 cells, respectively. Interestingly, the cell culture supernatants from VE6-TMPRSS2-H10  
294 cells yielded a positive result 3 to 5 cycles earlier than did the supernatants from Vero E6 cells,  
295 pointing to ~10-40 times more efficient virus production (Fig. S9). Altogether, infectious  
296 SARS-CoV-2 was recovered from all samples showing Ct values  $\leq 24.5$ . We then compared  
297 the antigen assay to virus isolation from the respective samples, and observed all of the samples  
298 with Ct values  $\leq 24.5$  to be positive in the NP assay (Fig. 2a). Of the samples with Ct values

299 >24.5 all produced a negative result in the TR-FRET NP assay, and SARS-CoV-2 was  
300 recovered from only one (Ct 24.87). By using the optimized conditions with 12 nM total labeled  
301 antibodies, the sensitivity of NP assay in comparison with virus isolation was 97.4% (37/38).  
302 The performance of the SP assay was poorer; only 8/38 samples with recoverable SARS-CoV-  
303 2 yielded a positive result (Fig. 2b).

#### 304 **False positivity and cross-reactivity**

305 After finding a total antibody concentration of 12 nM ideal for the assay performance, we  
306 were interested in knowing the rate of false positive results. To that end, we tested in the TR-  
307 FRET antigen assays 96 SARS-CoV-2 RT-PCR negative NPS samples. In parallel, we studied  
308 the potential cross-reactivity of cell culture grown seasonal common cold coronaviruses hCoV-  
309 229E and hCoV-NL63 in the TR-FRET assays. Among the SARS-CoV-2 RT-PCR negative  
310 NPS samples, only one produced a positive HTRF signal. We reanalyzed this sample with  
311 another RT-PCR assay (Xpert Xpress SARS-CoV-2, Cepheid), confirming the negative result.  
312 To assess the antigen-specificity of the signal, we also analyzed this sample using mismatching  
313 combinations of the labeled anti-NP and anti-RBD antibodies. All of the combinations yielded  
314 a positive result, suggesting that something other than the antigens bring the labeled antibodies  
315 together. By using the optimized conditions with 12 nM total labeled antibodies, the specificity  
316 of NP and SP TR-FRET assays in comparison with RT-PCR were 99.0% (95/96) and in  
317 comparison with virus isolation 100% (10/10). We then set as cutoffs for the TR-FRET assays  
318 the average plus four standard deviations of the signals from the SARS-CoV-2 RT-PCR  
319 negative NPS samples (excluding the single outlier). Using these cutoffs neither hCoV-229E  
320 nor hCoV-NL63 yielded a significant TR-FRET signal in either NP or SP assay (Fig. 3). The  
321 results with the cutoff values selected using the negative NPS samples concurred with those by  
322 the arbitrary cutoffs utilized earlier, and are summarized in Fig. 2.

## 323 **DISCUSSION**

324 The SARS-CoV-2 epidemic that began in China late 2019 quickly evolved into pandemic  
325 in the spring of 2020. After an initial lag in ramping up the testing capacity, RT-PCR quickly  
326 became the gold standard of acute SARS-CoV-2 diagnostics. While RT-PCR is very sensitive  
327 in picking up individuals with acute infection, the downside is that patients recovering from  
328 COVID-19 can remain RT-PCR positive over a long period. Antigen testing on the other hand  
329 is somewhat less sensitive for detecting the patients with acute infection; however, there  
330 appears to be a better correlation between presence of antigen and infectious virus in the NPS  
331 samples. In this manuscript, we describe a laboratory-developed test for the detection of SARS-  
332 CoV-2 antigen in NPS samples and compare the test's performance against virus isolation and  
333 RT-PCR. The assay is quick and very easy to use, furthermore the assay is rather uncomplicated  
334 to set up provided that specific antibodies against the structural proteins of the virus are  
335 available. While we employ polyclonal antibodies in the assay, it likely could be set up using  
336 monoclonals. The fluorophores (chelated Eu and AlexaFluor 647) are readily available, and  
337 the results can be read on any microplate reader capable of measuring time-resolved  
338 fluorescence. Notably, we set up the assay in detergent-containing RIPA buffer, which contains  
339 1% NP-40 and 0.1% SDS, both of which inactivate SARS-CoV-2<sup>21,22</sup>. Thus collecting the NPS  
340 samples directly into this matrix would significantly increasing the end user safety.

341 We set up the assay for the detection of both NP and SP of SARS-CoV-2 but observed a  
342 clear difference between the LODs of the two assays with NP being detected at approximately  
343 35 times lower concentration. This is likely explained by the fact that we employed an antibody  
344 directed against the RBD, which constitutes only about one sixth of SP. The fact that the  
345 antibody in use recognizes only a single domain could make it sterically impossible for two  
346 antibody molecules to bind a single SP molecule, and thus we speculate the obtained signal to  
347 come from SP trimers i.e. spikes. NP is more abundant in both virions and infected cells (refer



348 to Fig. S7), which additionally contributed to the higher sensitivity of NP detection in cell  
349 culture supernatants and NPS samples.

350 Performance analysis of the antigen assay using NPS samples from 48 SARS-CoV-2 RT-  
351 PCR positive and 96 negative individuals revealed that the NP assay correctly identified 37 of  
352 the positive samples, and all but one of the negatives. All the 37 true positives had a Ct value  
353 <25 cycles in the diagnostic RT-PCR. Similar to other studies, we observed a strong association  
354 between the sample infectivity and positive antigen test result; of the 38 samples that yielded  
355 an isolate 37 produced a positive result in the NP assay. We used 50  $\mu$ l for the virus isolation  
356 while the antigen assay only takes 10  $\mu$ l, which could explain why one of the samples with  
357 infectious virus was not picked up. We intentionally selected NPS samples over a broad range  
358 of Ct values in SARS-CoV-2 RT-PCR to obtain an estimate of the detection limit as compared  
359 to RT-PCR. The fact that we analyzed samples that were not collected fresh and had been  
360 subjected to at least one freeze-thaw cycle may have negatively affected the assay sensitivity.  
361 In any case, our test could detect 97.4% of the NPS samples with infectious virus.

362 Because both NP and SP antigen assays gave a positive result for a single SARS-CoV-2 RT-  
363 PCR negative sample, we re-analyzed it using a different RT-PCR with a negative result. We  
364 also attempted virus isolation from the sample but without success. It is possible that the false  
365 positive result is a result of cross-reactivity to a human coronavirus, hCoV, infection. Of the  
366 hCoVs only hCoV-NL63 and SARS-CoV use the same receptor as SARS-CoV-2, i.e. the  
367 angiotensin converting enzyme 2 (ACE2)<sup>24,25</sup>. Thus it would be most logical that the reactivity  
368 of this sample would be due to hCoV-NL63 because both SP (based on RBD) and NP assays  
369 gave a positive result. We did however test the two assays using cell culture -grown hCoV-  
370 229E and hCoV-NL63, yet with negative results. It appears that the sample yielding a false  
371 positive reaction contained an interfering substance, which caused the immunoglobulins to  
372 aggregate, because also labeled antibodies against different antigens yielded a TR-FRET



373 signal. The use of miss-matching antibodies could be in the future serve to discern true and  
374 false positives in the TR-FRET assay.

375 In conclusion, we report the development of a rapid SARS-CoV-2 antigen test based on  
376 simultaneous binding of two or more fluorophore-labeled antibody molecules to the antigen.  
377 The TR-FRET –based antigen test is rapid to perform, and its results correlate well with the  
378 presence of infectious virus in clinical sample. The assay is easy to set up, if a suitable antibody  
379 against SARS-CoV-2 NP and a plate reader enabling TR-FRET measurement are available.  
380 We estimate that a single plate reader and an experienced technician could manually analyze  
381 hundreds of specimens per hour, ideally with a 30-minute turn-around time from sample arrival  
382 to results (see supplementary information for details). The assay throughput could significantly  
383 be up scaled by using automation, and alike RT-PCR the sample collection would represent the  
384 major limiting factor. The NPS sampling directly to a detergent-containing buffer increases the  
385 assay’s user-safety. We envision that the assay could be applied widely in the field, e.g.  
386 hospitals, retirement homes, airports and train stations, and in schools to identify people likely  
387 to spread the virus.

388

389 **ACKNOWLEDGEMENTS**

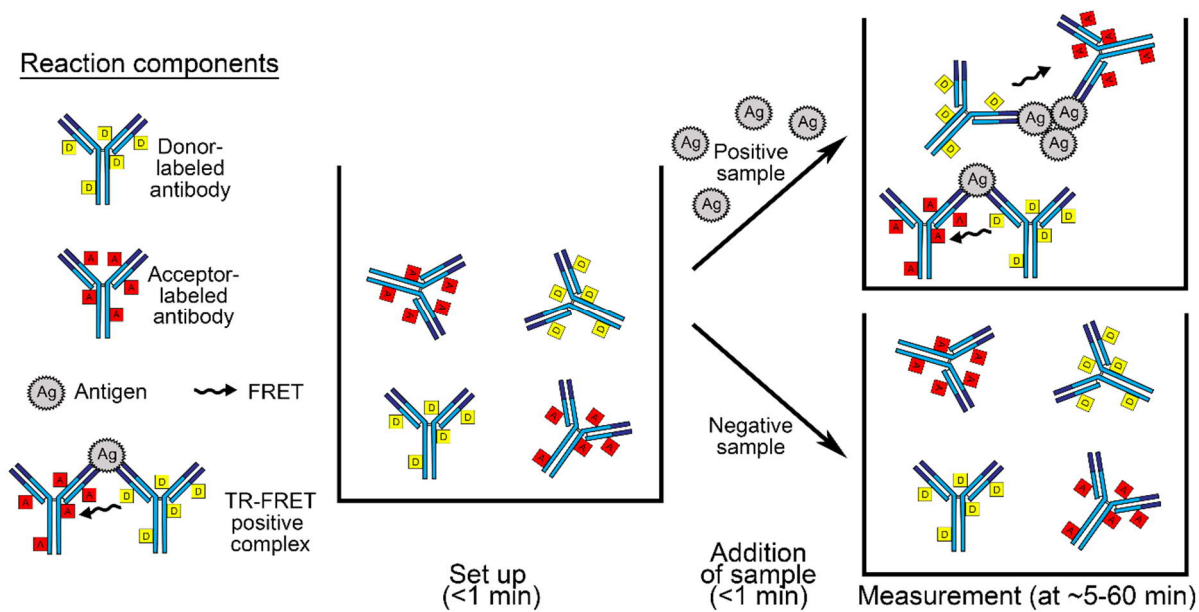
390 The authors wish to acknowledge Drs. Sisko Tauriainen (University of Turku, Turku,  
391 Finland) and Lia van der Hoek (Academic Medical Center, Amsterdam, Netherlands) for  
392 providing the human coronaviruses used for evaluating cross-reactivity. The study was  
393 supported by Academy of Finland (grants 308613, 314119, and 335762 to JH).

## 394 REFERENCES

- 395 1) Arons M.M. et al. Presymptomatic SARS-CoV-2 infections and transmission in a skilled  
396 nursing facility. *N Engl J Med* **382**, 2081-2090 (2020).  
397 <https://doi.org/10.1056/NEJMoa2008457>.
- 398 2) Bullard J. et al. Predicting Infectious SARS-CoV-2 From Diagnostic Samples. *Clin Infect*  
399 *Dis.* (2020) <https://doi.org/10.1093/cid/ciaa638>.
- 400 3) Wölfel R., et al. Virological assessment of hospitalized patients with COVID-2019. *Nature*  
401 **58**, 465-469 (2020) <https://doi.org/10.1038/s41586-020-2196-x>.
- 402 4) Pekosz A., et al. Antigen-based testing but not real-time PCR correlates with SARS-CoV-  
403 2 virus culture. *medRxiv* (2020). <https://doi.org/10.1101/2020.10.02.20205708>.
- 404 5) Mina M.J., et al. Rethinking Covid-19 Test Sensitivity - A Strategy for Containment. *N*  
405 *Engl J Med* **383**, e120 (2020). <https://doi.org/10.1056/NEJMp2025631>.
- 406 6) Dinnes J., et al. Rapid, point-of-care antigen and molecular-based tests for diagnosis of  
407 SARS-CoV-2 infection. *Cochrane Database Syst Rev* CD013705 (2020).  
408 <https://doi.org/10.1002/14651858.CD013705>.
- 409 7) U.S. Food and Drug Administration. Coronavirus Disease 2019 (COVID-19) Emergency  
410 Use Authorizations for Medical Devices: In Vitro Diagnostic EUAs. Updated 4.12.2020.  
411 Accessed 5.12.2020. [https://www.fda.gov/medical-devices/coronavirus-disease-2019-](https://www.fda.gov/medical-devices/coronavirus-disease-2019-covid-19-emergency-use-authorizations-medical-devices/vitro-diagnostics-euas)  
412 [covid-19-emergency-use-authorizations-medical-devices/vitro-diagnostics-euas](https://www.fda.gov/medical-devices/coronavirus-disease-2019-covid-19-emergency-use-authorizations-medical-devices/vitro-diagnostics-euas).
- 413 8) Saraheimo S., et al. Time-resolved FRET -based approach for antibody detection - a new  
414 serodiagnostic concept. *PLOS One* **8**, e62739 (2013)  
415 <https://doi.org/10.1371/journal.pone.0062739>.
- 416 9) Hepojoki S., et al. A protein L-based immunodiagnostic approach utilizing time-resolved  
417 Förster resonance energy transfer. *PLOS One* **9**, e106432 (2014).  
418 <https://doi.org/10.1371/journal.pone.0106432>.
- 419 10) Hepojoki S., et al. Rapid homogeneous immunoassay based on time-resolved Förster  
420 resonance energy transfer for serodiagnosis of acute hantavirus infection. *J Clin Microbiol*  
421 **53**, 636-640 (2015). <https://doi.org/10.1128/JCM.02994-14>.
- 422 11) Hepojoki S., et al. Competitive Homogeneous Immunoassay for Rapid Serodiagnosis of  
423 Hantavirus Disease. *J Clin Microbiol* **53**, 2292-2297 (2015).  
424 <https://doi.org/10.1128/JCM.00663-15>.
- 425 12) Kareinen L., et al. Immunoassay for serodiagnosis of Zika virus infection based on time-  
426 resolved Förster resonance energy transfer. *PLOS One* **14**, e0219474 (2019)  
427 <https://doi.org/10.1371/journal.pone.0219474>.
- 428 13) Rusanen J., et al. LFRET, a novel rapid assay for anti-tissue transglutaminase antibody  
429 detection. *PLOS One* **14**, e0225851 (2019). <https://doi.org/10.1371/journal.pone.0225851>.
- 430 14) Rusanen J., et al. Rapid homogeneous assay for detecting antibodies against SARS-CoV-  
431 2. *medRxiv* (2020). <https://doi.org/10.1101/2020.11.01.20224113>.

- 432 15) Mannonen L., et al. Comparison of two commercial platforms and a laboratory developed  
433 test for detection of SARS-CoV-2 RNA. *medRxiv* (2020).  
434 <https://doi.org/10.1101/2020.07.03.20144758>.
- 435 16) Corman V.M., et al. Detection of 2019 novel coronavirus (2019-nCoV) by real-time RT-  
436 PCR. *Euro Surveill* **25**, 2000045 (2020). [https://doi.org/10.2807/1560-](https://doi.org/10.2807/1560-7917.ES.2020.25.3.2000045)  
437 [7917.ES.2020.25.3.2000045](https://doi.org/10.2807/1560-7917.ES.2020.25.3.2000045).
- 438 17) Berthoux L., et al. Lvl1 Inhibition of Human Immunodeficiency Virus Type 1 Is  
439 Counteracted by Factors That Stimulate Synthesis or Nuclear Translocation of Viral cDNA.  
440 *J Virol* **78**, 11739-50 (2004). <https://doi.org/10.1128/JVI.78.21.11739-11750.2004>.
- 441 18) Haveri A., et al. Serological and molecular findings during SARS-CoV-2 infection: the first  
442 case study in Finland, January to February 2020. *Euro Surveill* **25**, 2000266 (2020).  
443 <https://doi.org/10.2807/1560-7917.ES.2020.25.11.2000266>.
- 444 19) Stadlbauer D., et al. SARS-CoV-2 Seroconversion in Humans: A Detailed Protocol for a  
445 Serological Assay, Antigen Production, and Test Setup. *Curr Protoc Microbiol* **57**, e100  
446 (2020). <https://doi.org/10.1002/cpmc.100>.
- 447 20) Amanat F., et al. A serological assay to detect SARS-CoV-2 seroconversion in humans.  
448 *Nat Med* **26**, 1033-1036 (2020). <https://doi.org/10.1038/s41591-020-0913-5>.
- 449 21) Welch S.R., et al. Analysis of Inactivation of SARS-CoV-2 by Specimen Transport Media,  
450 Nucleic Acid Extraction Reagents, Detergents, and Fixatives. *J Clin Microbiol* (2020)  
451 <https://doi.org/10.1128/JCM.01713-20>.
- 452 22) Patterson E.I., et al. Methods of Inactivation of SARS-CoV-2 for Downstream Biological  
453 Assays. *J Infect Dis* (2020). <https://doi.org/10.1093/infdis/jiaa507>.
- 454 23) Hoffman M., et al. SARS-CoV-2 Cell Entry Depends on ACE2 and TMPRSS2 and Is  
455 Blocked by a Clinically Proven Protease Inhibitor. *Cell* **181**, 271-280.e8 (2020).  
456 <https://doi.org/10.1016/j.cell.2020.02.052>.
- 457 24) Hofmann H., et al. Human coronavirus NL63 employs the severe acute respiratory  
458 syndrome coronavirus receptor for cellular entry. *Proc Natl Acad Sci* **102**, 7988–7993  
459 (2005). <https://doi.org/10.1073/pnas.0409465102>.
- 460 25) Li F. Receptor Recognition Mechanisms of Coronaviruses: a Decade of Structural Studies.  
461 *J Virol* **89**, 1954-64 (2015). <https://doi.org/10.1128/JVI.02615-14>.

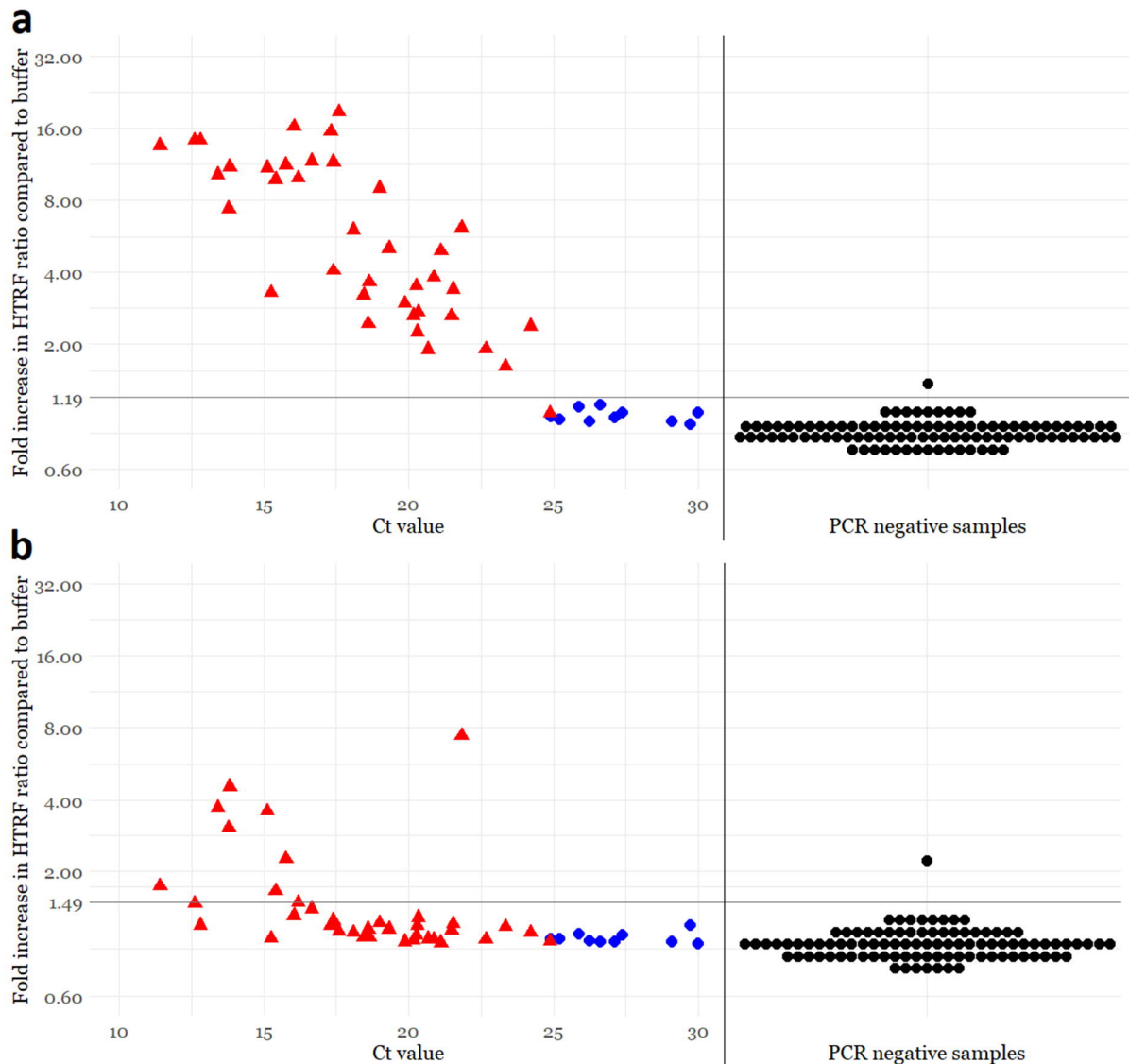
462 **FIGURES**



463

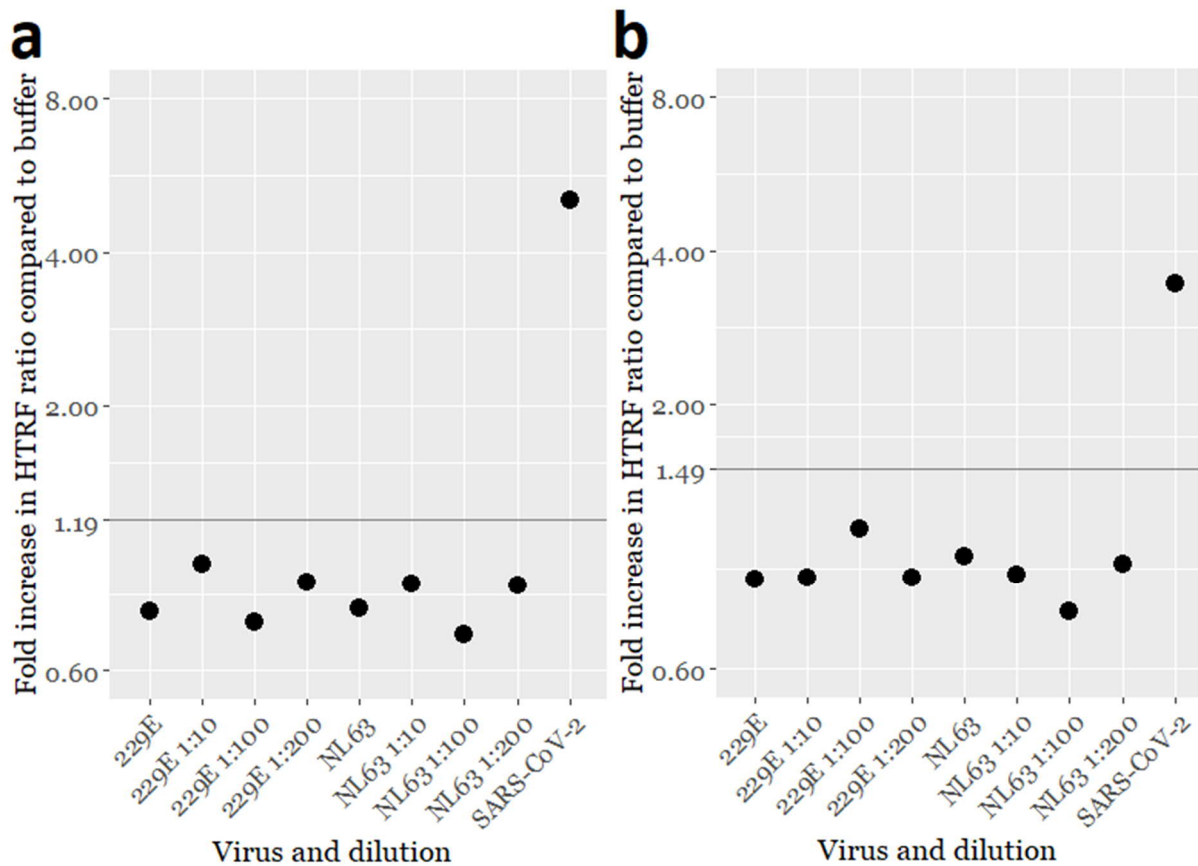
464 **Figure 1.** The TR-FRET assay workflow and principle. The left side shows the reaction  
465 components. At the center is a well containing donor- and acceptor-labeled antibodies at 1:1  
466 molar ratio in the reaction buffer, in our set up the total antibody concentration at this point is  
467 24 nM and the volume 10  $\mu$ l. The arrows indicate addition of the sample material, in our set up  
468 either 10  $\mu$ l of purified recombinant protein or 10  $\mu$ l of NPS sample. The top right side shows  
469 schematically the antigen-antibody complexes formed following addition of sample containing  
470 the antigen, reaction volume at this stage in our set up is 10  $\mu$ l. The bottom right side  
471 schematically demonstrates that the labelled antibodies do not form TR-FRET active  
472 complexes in absence of the antigen.

473



474

475 **Figure 2.** Comparison of TR-FRET based antigen detection and the amount of virus as  
476 analyzed by SARS-CoV-2 RT-PCR and virus isolation from NPS samples. The total antibody  
477 concentration in the assays is 12 nM (6 nM of Eu- and 6 nM of AF647-labeled antibody). a)  
478 Anti-NP assay results. b) Anti-RBD assay results. The y-axis (log scale) indicates a fold  
479 increase in HTRF ratio ( $HTRF_{\text{sample}}/HTRF_{\text{buffer}}$ ) measured directly after pipetting the samples  
480 on plate. The x-axis shows the Ct value measured in the diagnostic SARS-CoV-2 RT-PCR.  
481 The horizontal black line is the antigen test positivity cutoff, corresponding to the average plus  
482 four standard deviations of the signals induced by SARS-CoV-2 RT-PCR negative samples.  
483 The vertical black line separates SARS-CoV-2 RT-PCR positive (n = 48) and negative (n = 96)  
484 NPS samples. The coloring in the graphs indicates presence (red) or absence (blue) of  
485 cytopathic effect (CPE) following inoculation of VE6-TMPRSS2-H10 cells with 50  $\mu$ l of the  
486 NPS sample, black = not cultured. TR-FRET = time-resolved Förster resonance energy  
487 transfer, NP = nucleoprotein, RBD = receptor-binding domain, HTRF = homogeneous time-  
488 resolved fluorescence.



489

490 **Figure 3.** SARS-CoV-2 TR-FRET antigen assay cross-reactivity evaluated with cell culture  
491 supernatants of seasonal human coronaviruses hCoV-229E and -NL63. a) Anti-NP assay  
492 results with HCoV-229E and -NL63 cell culture supernatants at different dilutions. b) Anti-NP  
493 assay results with HCoV-229E and -NL63 cell culture supernatants at different dilutions. The  
494 y-axis (log scale) indicates a fold increase in HTRF ratio ( $HTRF_{\text{sample}}/HTRF_{\text{buffer}}$ ). The  
495 horizontal lines indicate the respective TR-FRET assay cutoffs. UV-inactivated SARS-CoV-2  
496 containing cell culture supernatant is included as a positive control.

497 **SUPPLEMENTARY INFORMATION**

498

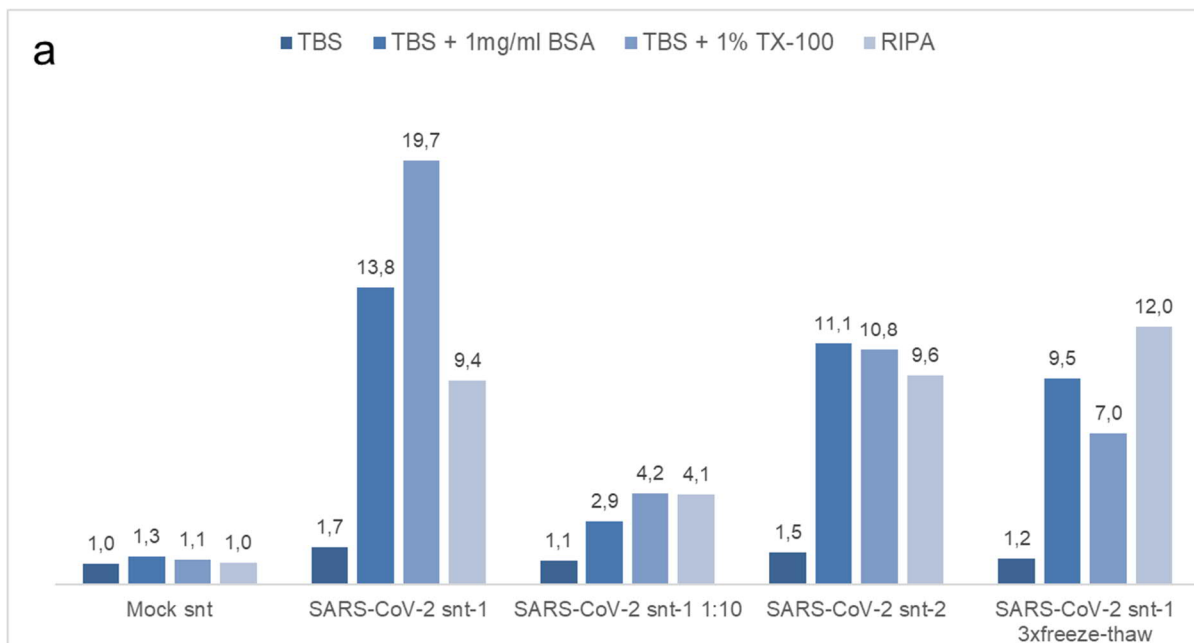
499 **Assay throughput estimate**

500 Using 384-well plates, 192 samples can be measured in duplicate on one plate. Pipetting the  
501 reagent mixes and samples manually on plate with a multichannel pipette is estimated to require  
502 10 minutes for a full plate (2-2.5 minutes for reagent mixes and 7.5-8 minutes for samples,  
503 longer for the latter due to tip change between samples). Measuring the HTRF ratio in triplicate  
504 takes approximately 18 min for a full 384-well plate using Hidex Sense (Hidex Oy, Finland).  
505 HTRF ratios are calculated automatically and the results can be exported as e.g. an Excel file.  
506 While the measurement takes place, the next plate can be prepared. With measurement intervals  
507 of 20 minutes, a single machine and one operator could ideally measure 576 samples/hour that  
508 would correspond to 13 824 samples/24 hours, assuming shift work. The throughput could be  
509 increased by including automation and additional staff to aid with sample preparation and the  
510 transfer of results to a laboratory information management system.

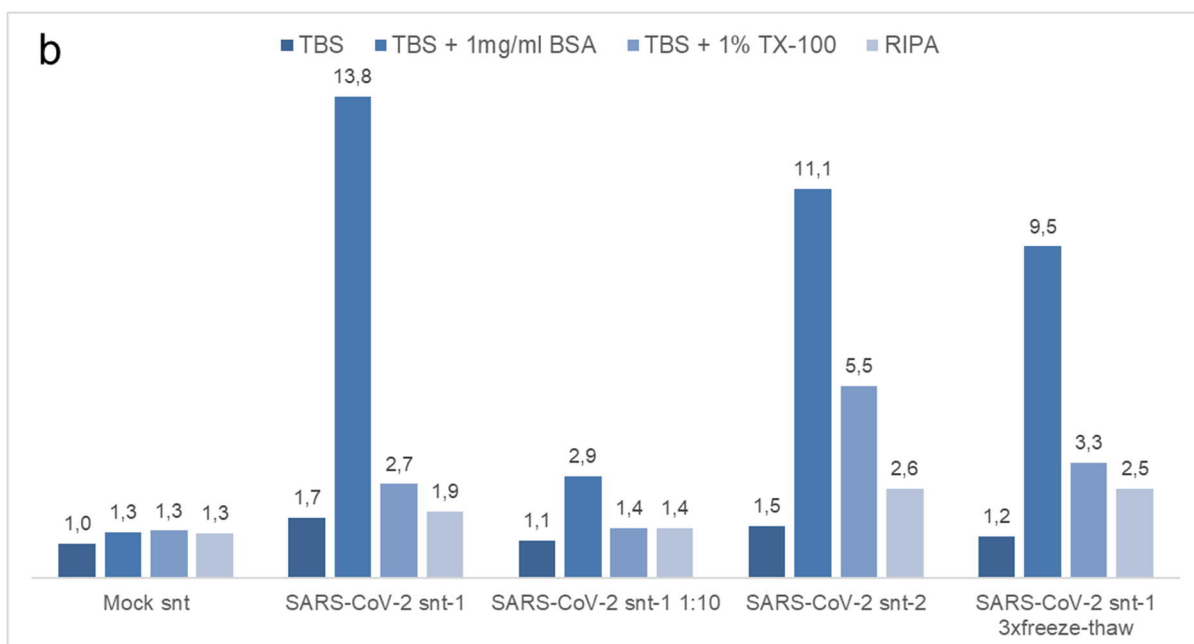


511 **Supplementary figures and tables**

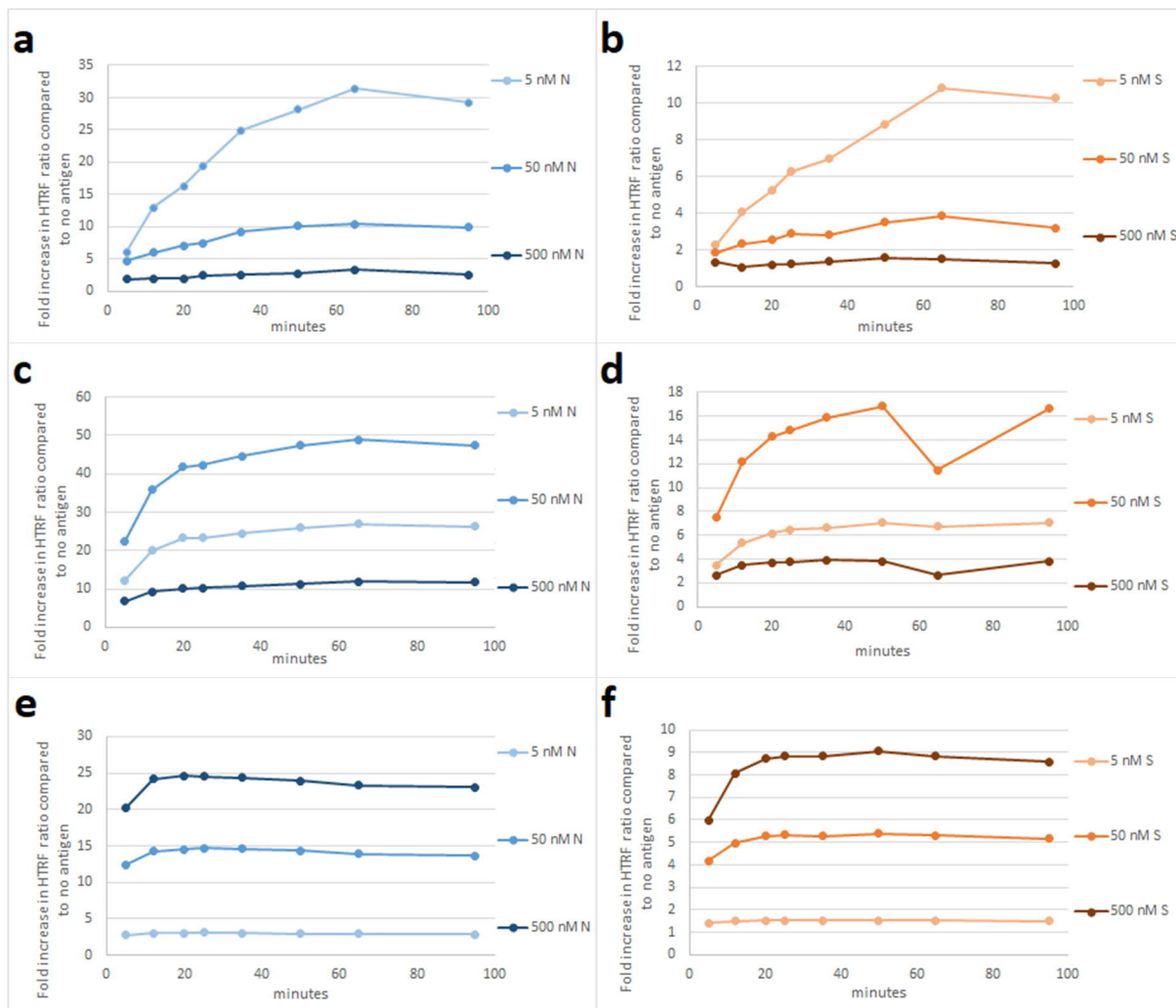
512



513



514 **Figure S1.** TR-FRET antigen assay in different buffer compositions. The antibody  
515 concentrations refer to the total amount used in reaction i.e. a 1:1 mixture of Eu- and AF647-  
516 labeled antibodies. a) Anti-NP at 1  $\mu$ M concentration. b) Anti-NP at 1  $\mu$ M concentration. The  
517 y-axis (and values over bars) indicates a fold increase in HTRF ratio ( $HTRF_{sample}/HTRF_{buffer}$ ).  
518 Mock snt = supernatant from mock-infected Vero E6 cells, SARS-CoV-2 snt-1 and -2 =  
519 supernatants containing infectious SARS-CoV-2.



520

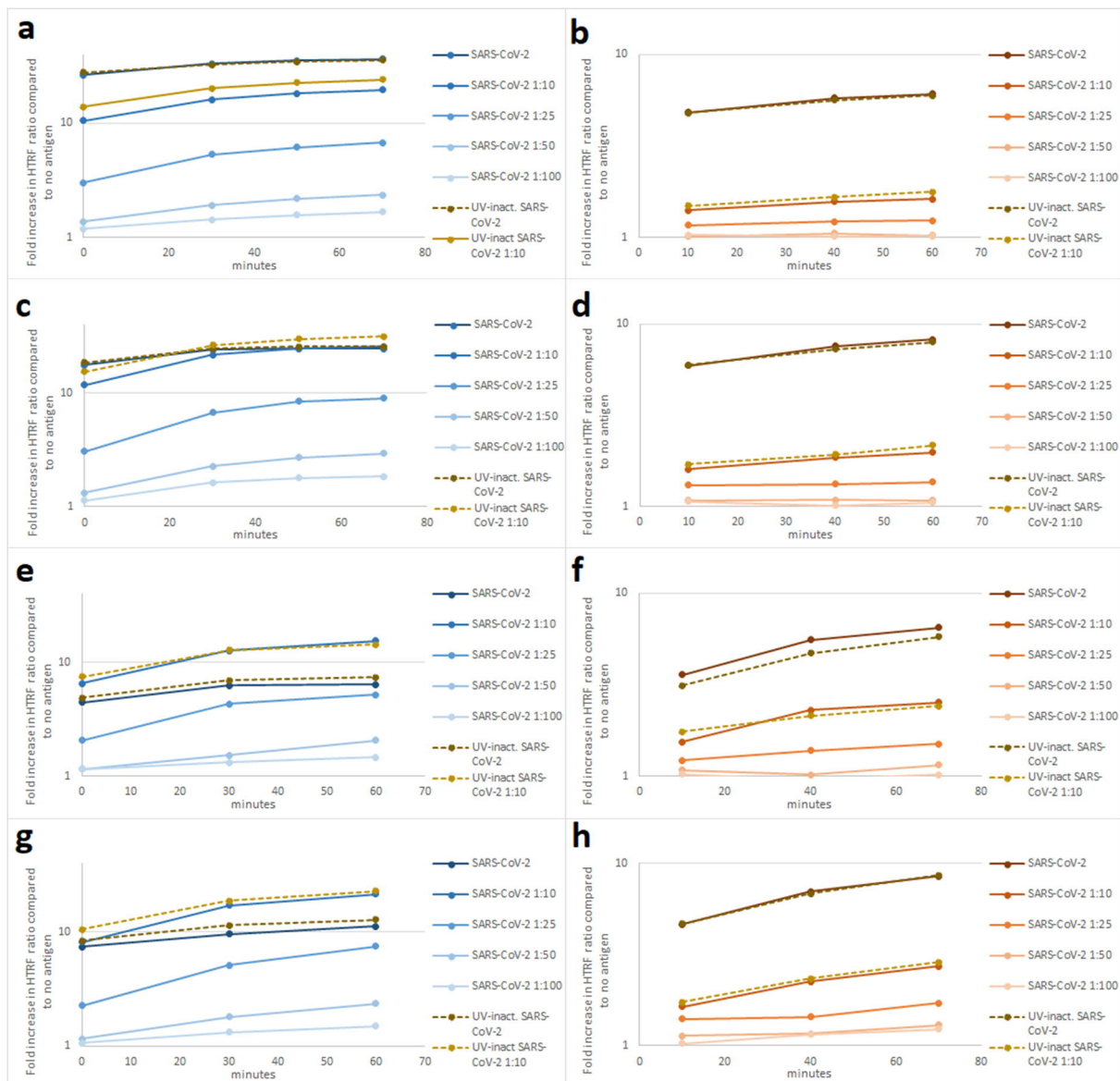
521 **Figure S2.** TR-FRET cross-titration of labeled antibodies and purified recombinant NP and  
522 SP. a) Anti-NP antibody concentration of 5 nM against NP concentrations of 5, 50 and 500  
523 nM. b) Anti-RBD antibody concentration of 5 nM against SP concentrations of 5, 50 and 500  
524 nM. c) Anti-NP antibody concentration of 50 nM against NP concentrations of 5, 50 and 500  
525 nM. d) Anti-RBD antibody concentration of 50 nM against SP concentrations of 5, 50 and 500  
526 nM. e) Anti-NP antibody concentration of 500 nM against NP concentrations of 5, 50 and 500  
527 nM. f) Anti-RBD antibody concentration of 500 nM against SP concentrations of 5, 50 and 500  
528 nM. The antibody concentrations refer to the total amount used in reaction i.e. a 1:1 mixture of  
529 Eu- and AF647-labeled antibodies. The y-axis indicates a fold increase in HTRF ratio  
530 ( $HTRF_{\text{sample}}/HTRF_{\text{buffer}}$ ). The x-axis shows time in minutes since the pipetting of the samples  
531 on plate began (~5 minutes before the first measurement). NP = nucleoprotein, SP = spike  
532 glycoprotein, RBD = receptor-binding domain.

533

534 **Table S1.** Comparison of TR-FRET antigen assay results, expressed as HTRF ratio  
 535 (HTRF<sub>sample</sub>/HTRF<sub>buffer</sub>), using different ratios of Eu- and AF647-labeled anti-NP and anti-  
 536 RBD antibodies. NP = nucleoprotein, RBD = receptor-binding domain, Eu = Eu-labeled, AF =  
 537 Alexa Fluor 647 labeled.

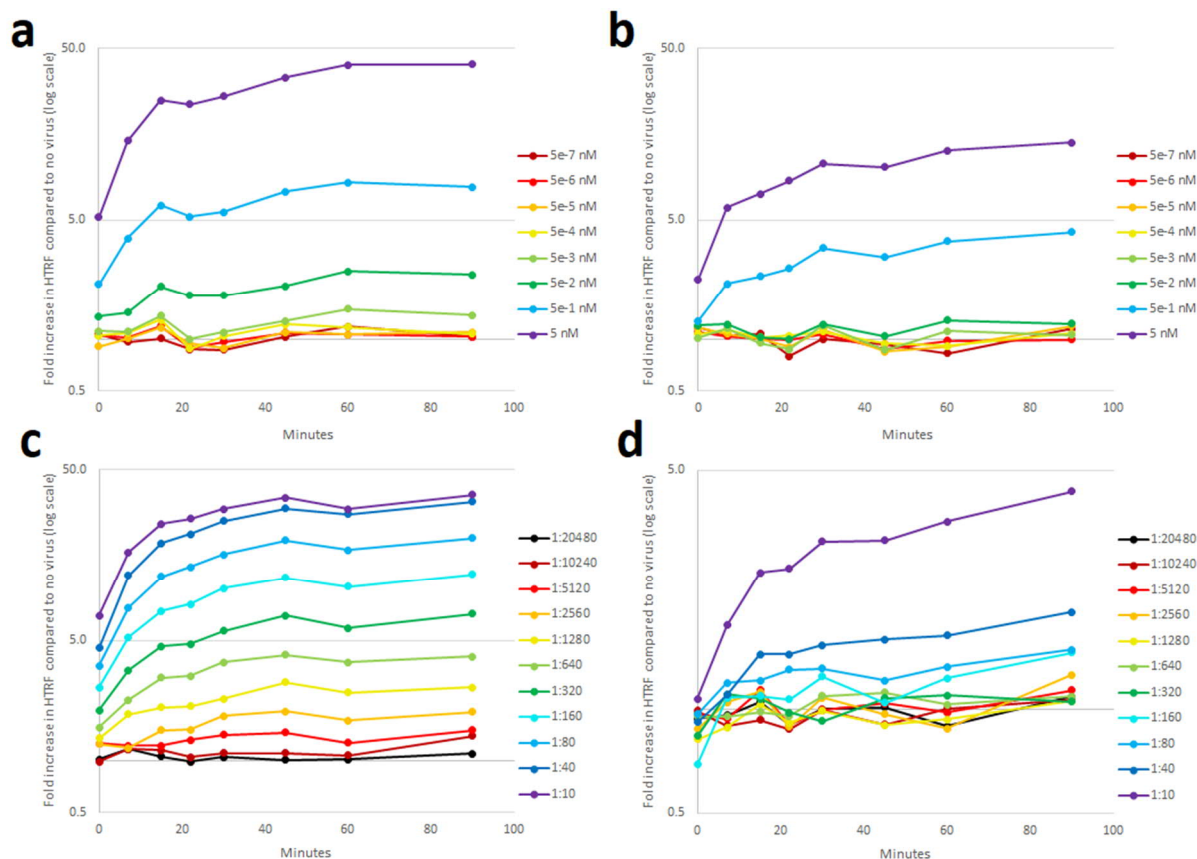
	HTRF ratio compared to average of mock media 1:1 and 1:100								
	10 µl VE6					10 µl VE6 mock-media			
	1:1	1:10	1:50	1:100	1:1000	1:1	1:100		
anti-NP 10 nM Eu + 10 nM AF	18.8	15.9	4.4	2.7	1.2	1.0	1.0		
anti-NP 20 nM Eu + 20 nM AF	26.1	12.8	3.7	2.5	1.2	1.0	1.0		
anti-NP 40 nM Eu + 40 nM AF	45.0	10.4	2.9	2.1	1.1	1.0	1.0		
anti-NP 80 nM Eu + 80 nM AF	39.5	7.0	2.2	1.7	1.1	1.0	1.0		
anti-NP 13 nM Eu + 27 nM AF	23.0	16.5	4.5	2.8	1.2	1.0	1.0		
anti-NP 27 nM Eu + 13 nM AF	13.0	14.9	4.5	2.8	1.2	1.0	1.0		
anti-RBD 10 nM Eu + 10 nM AF	3.6	1.3	1.3	1.1	1.1	1.0	1.0		
anti-RBD 20 nM Eu + 20 nM AF	3.3	1.3	1.1	1.0	1.0	1.0	1.0		
anti-RBD 40 nM Eu + 40 nM AF	2.7	1.2	1.1	1.0	1.0	1.0	1.0		
anti-RBD 80 nM Eu + 80 nM AF	2.3	1.2	1.0	1.0	1.0	1.0	1.0		
anti-RBD 13 nM Eu + 27 nM AF	3.1	1.2	1.0	1.0	0.9	1.0	1.0		
anti-RBD 27 nM Eu + 13 nM AF	2.3	1.1	1.0	1.1	1.0	1.0	1.0		

538



539

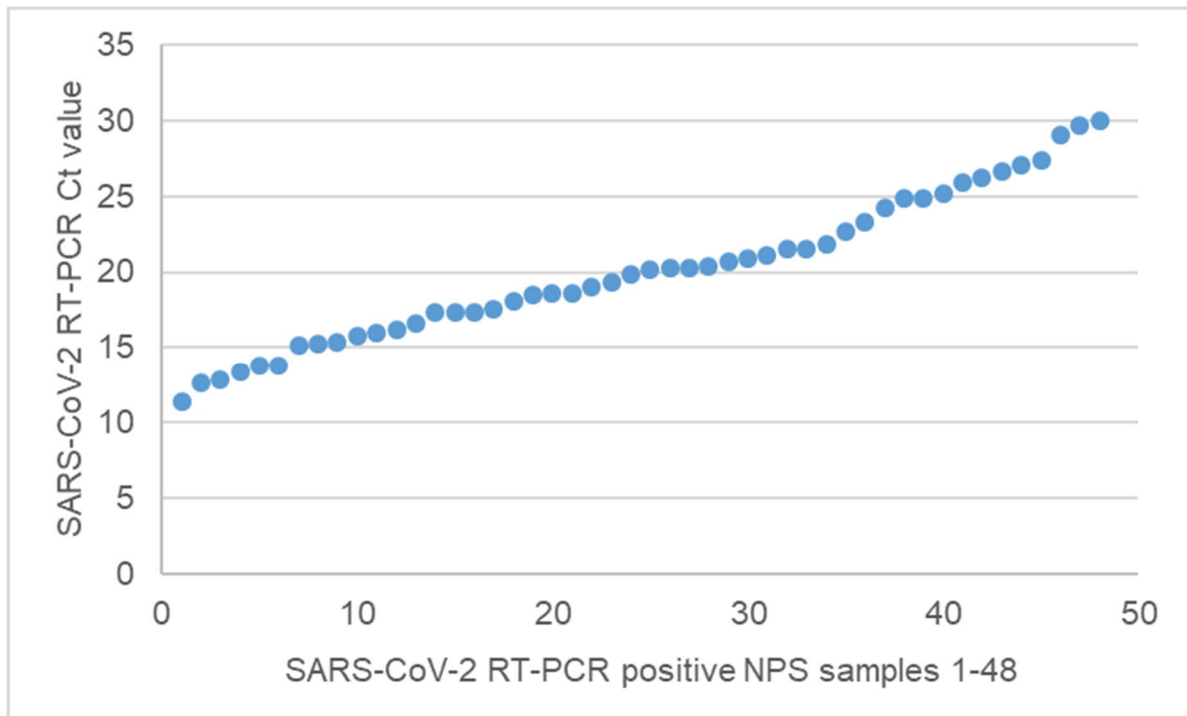
540 **Figure S3.** TR-FRET cross-titration of labeled antibodies and virus-containing cell culture  
 541 supernatants. The antibody concentrations refer to the total amount used in reaction i.e. a 1:1  
 542 mixture of Eu- and AF647-labeled antibodies. The different antibody concentrations were  
 543 titrated against SARS-CoV-2 containing cell culture supernatant spiked at varying dilutions in  
 544 a pool of negative NPS samples. a) Anti-NP antibody at 50 nM. b) Anti-RBD antibody at 50  
 545 nM. c) Anti-NP antibody at 25 nM. d) Anti-RBD antibody at 25 nM. e) Anti-NP antibody at  
 546 12 nM. f) Anti-RBD antibody at 12 nM. g) Anti-NP antibody at 6 nM. h) Anti-RBD antibody  
 547 at 6 nM. The y-axis (log scale) indicates a fold increase in HTRF ratio ( $HTRF_{sample}/HTRF_{buffer}$ ).  
 548 The x-axis shows time in minutes since the first measurement began.



549

550 **Figure S4.** The limit of detection for TR-FRET antigen detection using NPS samples spiked  
 551 with recombinant antigens or inactivated virus. The evaluation is with total antibody  
 552 concentrations of 12 nM, i.e. 6 nM of Eu- and 6 nM of AF647-labeled antibodies. a)  
 553 Recombinant NP spiked at 0.5 fM to 5 nM in a pool of negative NPS samples. b) Recombinant  
 554 SP spiked at 0.5 fM to 5 nM in a pool of negative NPS samples. c) UV inactivated SARS-CoV-  
 555 2 containing cell culture supernatant spiked at 1:20480 to 1:10 in a negative NP swab sample,  
 556 with labeled anti-N antibodies at 6+6 nM. d) Inactivated SARS-CoV-2 spiked at 1:20480 to  
 557 1:10 in a pool of negative NPS samples. The y-axis (log scale) indicates a fold increase in  
 558 HTRF ratio ( $HTRF_{\text{sample}}/HTRF_{\text{buffer}}$ ). The x-axis shows time in minutes since the first  
 559 measurement began. NP = nucleoprotein, SP = spike glycoprotein, RBD = receptor-binding  
 560 domain.

561

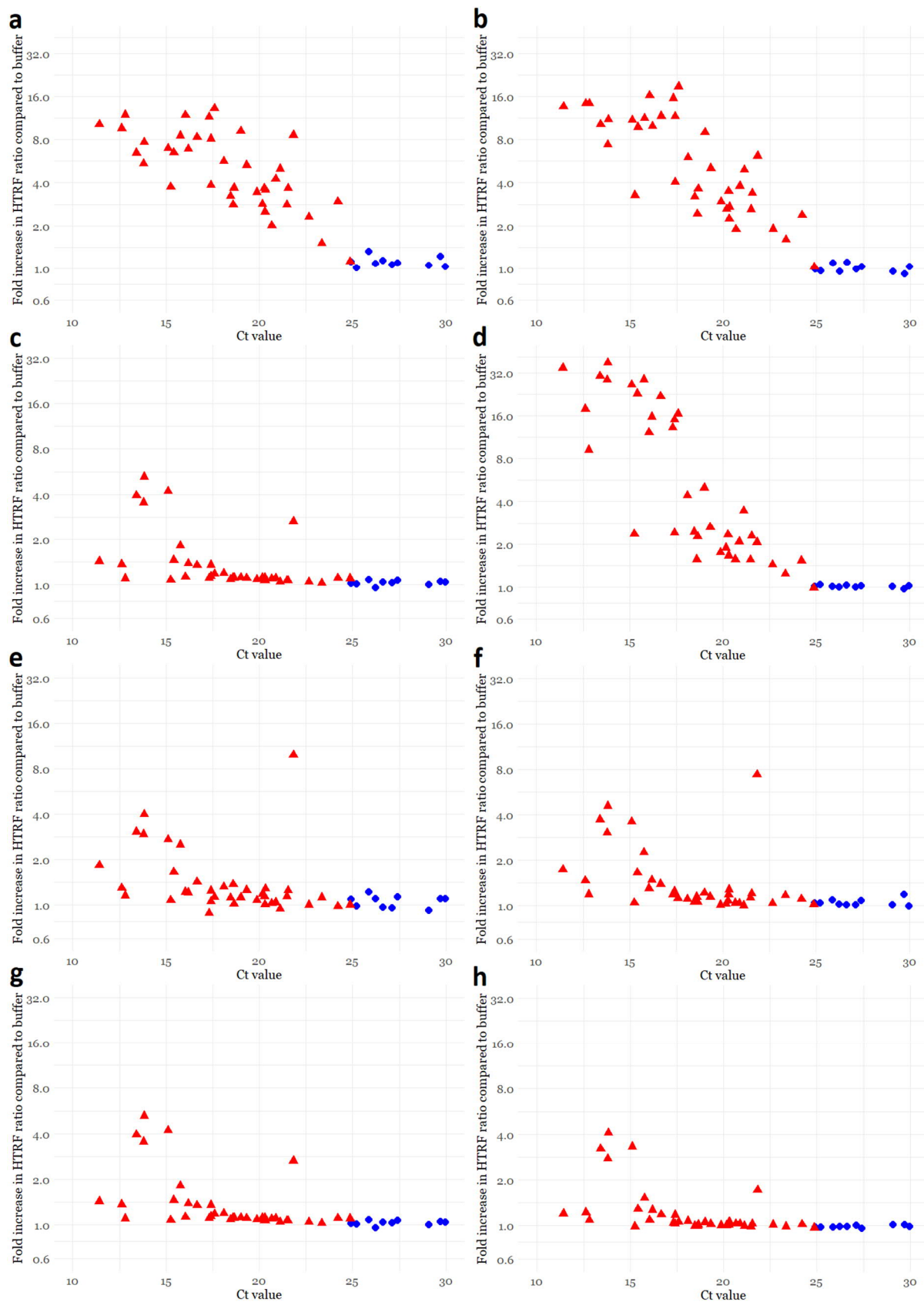


562

563 **Figure S5.** Distribution of the Ct values in the original diagnostic SARS-CoV-2 RT-PCR. The  
564 y-axis shows the Ct value in the RT-PCR and X-axis shows the sample number.

565



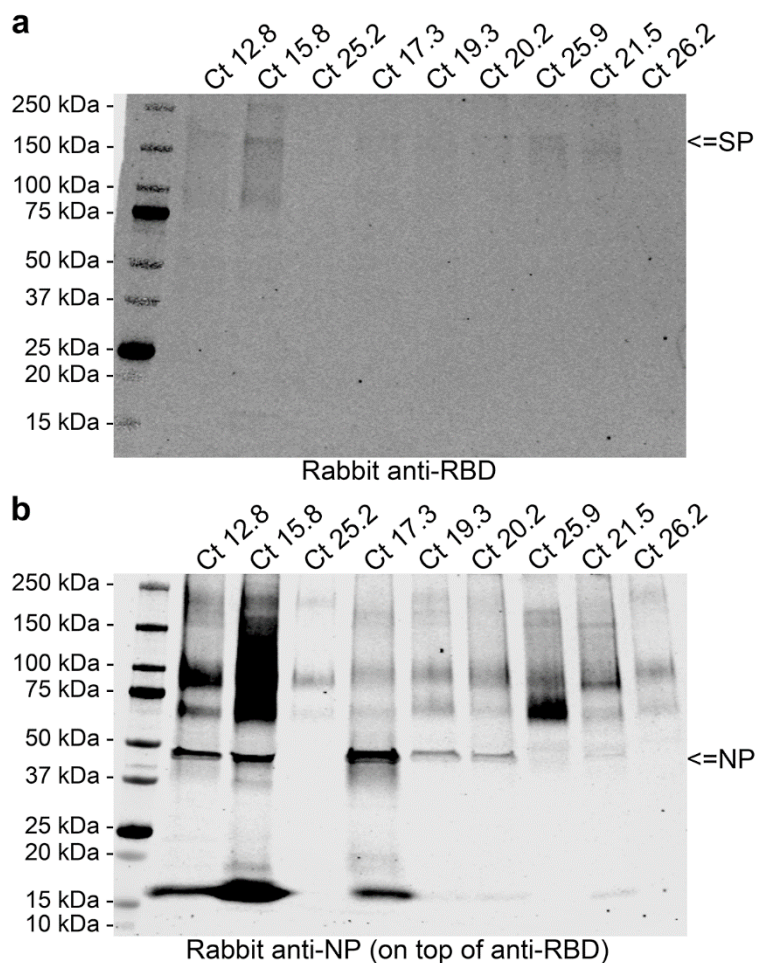


566

567 **Figure S6.** TR-FRET antigen assay results for NPS samples at varying antibody concentrations  
568 (6 to 50 nM) against Ct value of the positive SARS-CoV-2 RT-PCR result. a) Anti-NP antibody  
569 at 6 nM concentration. b) Anti-NP antibody at 12 nM concentration. c) Anti-NP antibody at  
570 25 nM concentration. d) Anti-NP antibody at 50 nM concentration. e) Anti-RBD antibody at

571 6 nM concentration. f) Anti-RBD antibody at 12 nM concentration. g) Anti-RBD antibody at  
572 25 nM concentration. h) Anti-RBD antibody at 50 nM concentration. The y-axis (log scale)  
573 indicates a fold increase in HTRF ratio ( $HTRF_{\text{sample}}/HTRF_{\text{buffer}}$ ) measured directly after  
574 pipetting of the samples on plate. The x-axis shows the Ct value measured in the diagnostic  
575 SARS-CoV-2 RT-PCR. The coloring in the graphs indicates presence (red) or absence (blue)  
576 of cytopathic effect (CPE) following inoculation of VE6-TMPRSS2-H10 cells with 50  $\mu$ l of  
577 the NPS sample. FRET = Förster resonance energy transfer, NP = nucleoprotein, RBD =  
578 receptor-binding domain, Ct = cycle threshold, Eu = europium, AF = Alexa Fluor 647.  
579

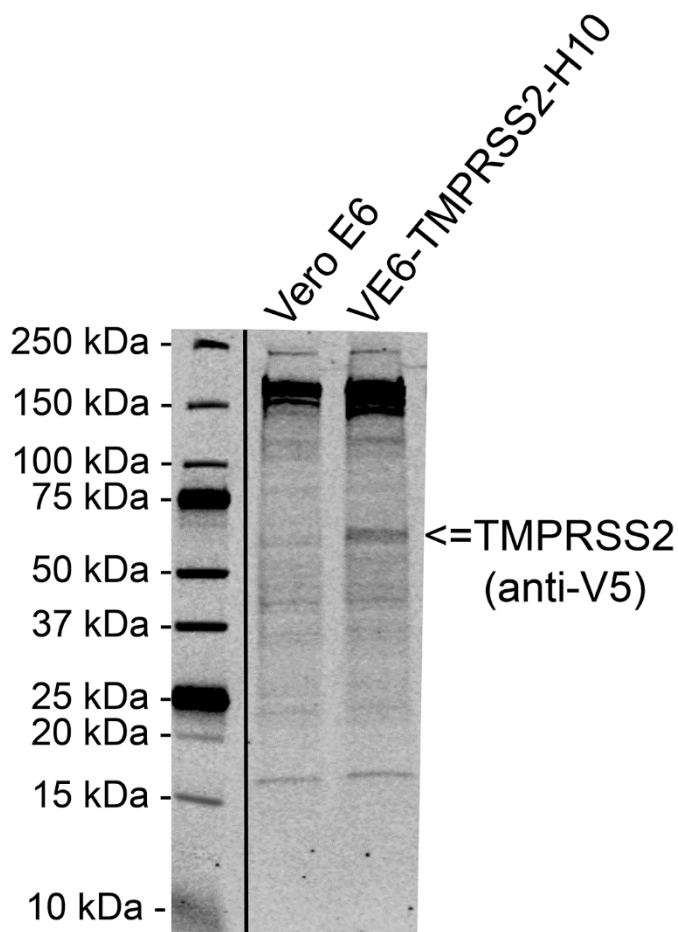




580

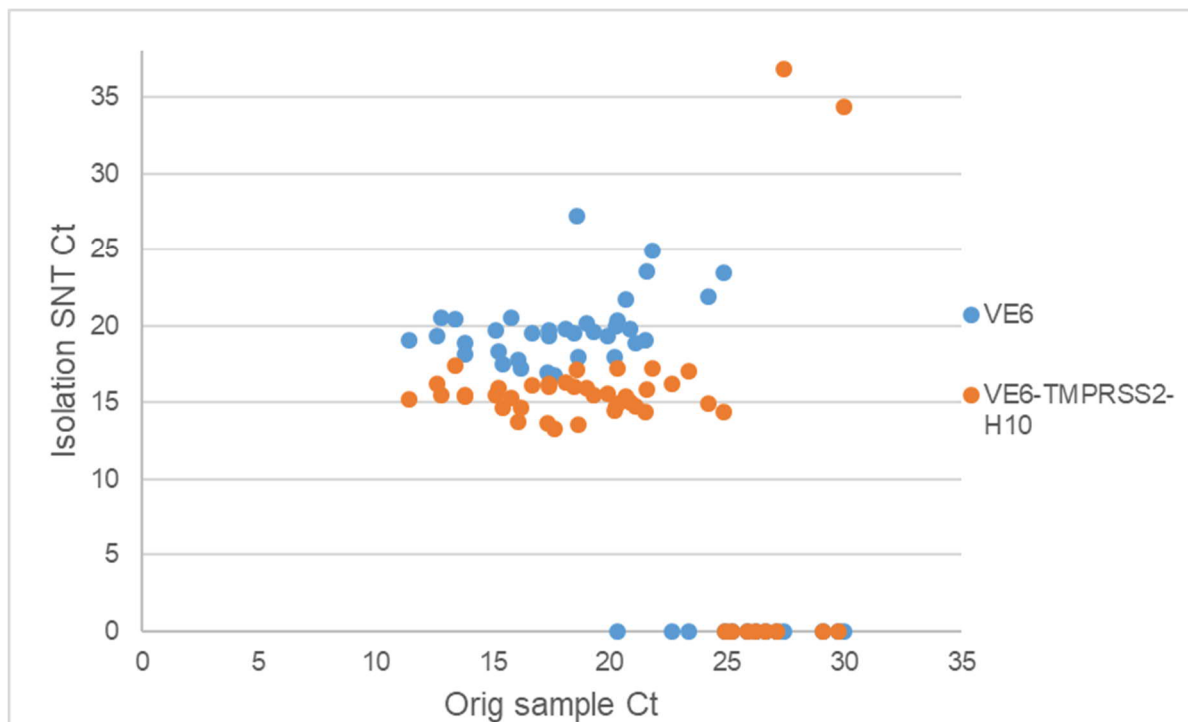
581 **Figure S7.** Detection of SARS-CoV-2 antigens in selected NPS samples by immunoblotting.  
582 The NPS samples selected based on the Ct values in the diagnostic SARS-CoV-2 RT-PCR  
583 were separated on SDS-PAGE (4-15% Mini-PROTEAN TGX Precast Protein Gel, deep well,  
584 Bio-RAD), approximately 40  $\mu$ l of NPS sample/well, using standard protocol but under non-  
585 reducing conditions. The proteins transferred (standard wet blotting protocol) onto  
586 nitrocellulose membrane (Nitrocellulose Blotting Membrane, Amersham Protran 0.45  $\mu$ m NC,  
587 GE Healthcare) were following blocking (30 min at room temperature, blocking buffer: 3%  
588 skimmed milk powder in 50 mM Tris, 150 mM NaCl, 0.05% Tween 20) first probed with anti-  
589 RBD antiserum (1:3000 diluted in blocking buffer), and the binding detected using IRDye  
590 800CW Donkey anti-rabbit IgG secondary antibody (LI-COR Biosciences), 1:10000 dilution  
591 in blocking buffer. The membrane was then probed with anti-NP antiserum (1:4000 diluted in  
592 blocking buffer), and the same secondary antibody was used for the detection. The results were  
593 recorded using Odyssey Infrared Imaging System (LI-COR Biosciences). **a**) The result of anti-  
594 RBD (detects S protein under non-reducing conditions) staining. The wells are labeled by the  
595 diagnostic SARS-CoV-2 RT-PCR values of the NPS samples. A band migrating at  
596 approximately 170 kDa (indicated by an arrow) represents the unprocessed SP and it is detected  
597 in some of the samples. **b**) The result of anti-NP staining. The labeling of wells as in **a**. A band  
598 migrating at approximately 45 kDa (indicated by an arrow) represents the NP and it is clearly  
599 detectable in samples with Ct values <21.5.

600



601

602 **Figure S8.** Detection of Transmembrane serine protease 2 (TMPRSS2) in the clonal population  
603 of lentivirus-transduced Vero E6 cells expressing TMPRSS2 (VE6-TMPRSS2-H10). Wild-  
604 type Vero E6 and VE6-TMPRSS2-H10 cells were collected from a 6-well plate using cell  
605 scraper, washed twice with PBS, and lysed in Laemmli Sample Buffer. The cell lysates were  
606 separated on SDS-PAGE (4-20% Mini-PROTEAN TGX Precast Protein Gel, Bio-RAD),  
607 using standard protocol. The proteins transferred (standard wet blotting protocol) onto  
608 nitrocellulose membrane (Nitrocellulose Blotting Membrane, Amersham Protran 0.45  $\mu$ m NC,  
609 GE Healthcare) were following blocking (30 min at room temperature, blocking buffer: 3%  
610 skimmed milk powder in 50 mM Tris, 150 mM NaCl, 0.05% Tween 20) probed with mouse  
611 monoclonal anti-V5 epitope tag antibody (clone E10/V4RR, Invitrogen), diluted 1:2000 in  
612 blocking buffer. The binding was detected using IRDye 800CW Donkey anti-mouse IgG  
613 secondary antibody (LI-COR Biosciences), 1:10000 dilution in blocking buffer, and the results  
614 were recorded using Odyssey Infrared Imaging System (LI-COR Biosciences). The band  
615 indicated by an arrow at approximately 60-65 kDa by migration indicates the expression of  
616 V5-tagged TMPRSS2 by the VE6-TMPRSS2-H10 clone of Vero E6.



617

618 **Figure S9.** RT-PCR results from supernatants collected at 5 days post inoculation with SARS-  
619 CoV-2 RT-PCR positive NPS samples. Y-axis shows Ct value from SARS-CoV-2 RT-PCR  
620 from the cell culture supernatant and X-axis shows the respective Ct value of the original  
621 diagnostic test. The blue dots indicate supernatant from isolation attempt on Vero E6 cells  
622 and the orange dots indicate supernatant from isolation attempt on VE6-TMRPRSS2-H10 cells.

623